


Brain structural profile of multiple system atrophy patients with cognitive impairment

Eleonora Fiorenzato^{1,2}  · Luca Weis¹ · Klaus Seppi³ · Marco Onofri⁴ · Pietro Cortelli^{5,6} · Stefano Zanigni^{6,7} · Caterina Tonon^{6,7} · Horacio Kaufmann⁸ · Timothy Michael Shepherd⁸ · Werner Poewe³ · Florian Krismer³ · Gregor Wenning³ · Angelo Antonini¹ · Roberta Biundo¹ · On behalf of the Movement Disorders Society MSA (MODIMSA) Neuropsychology and Imaging Study Groups

Received: 25 September 2016 / Accepted: 17 October 2016 / Published online: 24 October 2016
© Springer-Verlag Wien 2016

Abstract Current consensus diagnostic criteria for multiple system atrophy (MSA) consider dementia a non-supporting feature, although cognitive impairment and even frank dementia are reported in clinical practice. Mini-Mental State Examination (MMSE) is a commonly used global cognitive scale, and in a previous study, we established an MSA-specific screening cut-off score <27 to identify cognitive impairment. Finally, MSA neuroimaging findings suggest the presence of structural alterations in patients with cognitive deficits, although the extent of the anatomical changes is unclear. The aim of our multicenter study is to better characterize anatomical

changes associated with cognitive impairment in MSA and to further investigate cortical and subcortical structural differences versus healthy controls (HC). We examined retrospectively 72 probable MSA patients [50 with normal cognition (MSA-NC) and 22 cognitively impaired (MSA-CI) based on MMSE <27] and compared them to 36 HC using gray- and white-matter voxel-based morphometry and fully automated subcortical segmentation. Compared to HC, MSA patients showed widespread cortical (bilateral frontal, occipito-temporal, and parietal areas), subcortical, and white-matter alterations. However, MSA-CI showed only focal volume reduction in the left dorsolateral prefrontal cortex compared with MSA-NC. These results suggest only a marginal contribution of cortical pathology to cognitive deficits. We believe that cognitive dysfunction is driven by focal fronto-striatal degeneration in line with the concept of “subcortical cognitive impairment”.

Keywords Multiple system atrophy (MSA) · Cognition · Mini-Mental State Examination (MMSE) · Dementia · Neuroimaging · Voxel-based morphometry

Introduction

Multiple system atrophy (MSA) is characterized by progressive neuronal degeneration and glial cytoplasmic inclusions in the cerebellum, pontine nuclei, inferior olivary nucleus, striatum, and substantia nigra (Quinn 1989). MSA patients present with autonomic failure as well as rapid progressive parkinsonism (MSA-P) and/or cerebellar ataxia (MSA-C) (Gilman et al. 2008). A few years after disease onset, the clinical and pathological features of MSA-C and MSA-P frequently overlap (Antonini et al.

✉ Eleonora Fiorenzato
eleonora.fiorenzato@gmail.com

- ¹ Parkinson Disease and Movement Disorders Unit, IRCCS San Camillo Hospital Foundation, via Alberoni, 70, 30126 Venice-Lido, Italy
- ² Department of General Psychology, University of Padua, via Venezia, 8, 35131 Padua, Italy
- ³ Department of Neurology, Medical University of Innsbruck, Anichstraße, 35, 6020 Innsbruck, Austria
- ⁴ Department of Neuroscience, Imaging and Clinical Sciences, “G. d’Annunzio” University, via dei Vestini, 33, 66100 Chieti, Italy
- ⁵ IRCCS Institute of Neurological Sciences of Bologna, via Altura, 3, 40139 Bologna, Italy
- ⁶ Department of Biomedical and Neuromotor Sciences (DIBINEM), University of Bologna, via Ugo Foscolo, 7, 40123 Bologna, Italy
- ⁷ Functional MR Unit, S. Orsola-Malpighi Hospital, via Massarenti, 9, 40138 Bologna, Italy
- ⁸ Department of Neurology, Dysautonomia Center, New York University, 530 First Avenue, Suite 9Q, New York, NY 10016, USA

1998; Ciolli et al. 2014; Colosimo et al. 2001; Wenning et al. 1995).

In the current diagnostic consensus criteria, the presence of cognitive dysfunction or dementia is considered a non-supporting feature (Gilman et al. 2008), but there is growing evidence that MSA patients often experience executive dysfunction or multiple cognitive deficits (Asi et al. 2014; Auzou et al. 2015; Stankovic et al. 2014). In a large multicenter study, we diagnosed dementia in approximately 12% of MSA patients based on daily functioning and a full neuropsychological battery. Based on this categorization, we also defined a screening MMSE cut-off score for MSA dementia with high specificity and sensitivity (96.9 and 84.6%) (Auzou et al. 2015).

Magnetic resonance imaging (MRI) findings suggest discrete cortical and subcortical abnormalities in MSA with cognitive deficits (Kim et al. 2015; Lee et al. 2016), although these studies were single center and collected in a relatively small number of patients at various stages of disease.

The objective of this multicenter study is to investigate anatomical alterations in MSA patients with cognitive impairment defined as MMSE < 27 cut-off score, and to further characterize cortical and subcortical structural differences versus healthy controls (HC).

Since MRI voxel-based morphometry (VBM) is not designated for the analysis of subcortical structures, we used a multimodal approach with fully automated segmentation of gray-matter nuclei.

Methods

Participants and centers

A cohort of 72 probable MSA patients was retrospectively collected from five international movement disorders centers; IRCCS San Camillo Hospital Foundation, Venice-Lido, Italy, $n = 34$; Clinical Department of Neurology, Innsbruck Medical University, Innsbruck, Austria, $n = 18$; IRCCS Institute of Neurological Sciences of Bologna, Bologna, Italy, $n = 7$; Department of Neuroscience, Imaging and Clinical Sciences, “G. d’Annunzio” University, Pescara, Italy, $n = 7$; Dysautonomia Center, Department of Neurology, New York University School of Medicine, New York, USA, $n = 6$. Data were compared with 36 HC collected at the Parkinson Unit in Venice, and matched for age and education. MSA and HC participants were scanned between 2010 and 2015. The study received ethical approval by the Venice Research Ethics Committee, Venice, Italy. The research was completed in accordance with the Helsinki Declaration.

Clinical assessment

Clinical and MRI data were available for all participants. Diagnosis of probable MSA was made by expert neurologists, based on clinical history and neurological examination according to established criteria (Gilman et al. 2008). We included individuals without significant cortical or white-matter vascular lesions of grades 2 and 3 (as seen on T2-weighted axial and T2-weighted fluid attenuation inversion recovery), or motion artifacts (Schmidt et al. 2003).

The following clinical characteristics were assessed: gender, education, age at onset and at examination, disease duration, and disease severity measured with the motor section of the Movement Disorder Society Unified Parkinson Disease Rating Scale (MDS-UPDRS III). Global cognitive functioning was assessed with the MMSE performed within 4 weeks of MRI (Folstein et al. 1975). Based on our previous MSA study, the presence of cognitive impairment was defined as MMSE score < 27 (Auzou et al. 2015). We then identified two subgroups according to this MMSE cut-off score: MSA with normal cognition (MSA-NC) and MSA cognitively impaired (MSA-CI).

Since our cohort consisted of patients in the moderate to advanced stages of the disease, which at time of examination presented with a combination of parkinsonism and cerebellar features in addition to autonomic dysfunction, we did not analyze separately MSA-C and MSA-P (Antonini et al. 1998; Ciolli et al. 2014; Colosimo et al. 2001; Wenning et al. 1995). However, individual demographic and clinical details are reported in the Online Resource 1.

MRI imaging protocols

In 66 patients and 36 HC, brain MRI was acquired on a 1.5T and in 6 on a 3T scanner according to centers’ routine acquisition protocols (see Online Resource 2 for T1-weighted 3D volumetric parameter details).

Voxel-based morphometry analysis

Structural data were analyzed with FSL-VBM, a VBM pipeline, carried out with FSL tools (Jenkinson et al. 2012). First, structural images were brain-extracted using the Brain Extraction Tool (BET) after image z direction-cropping at medulla level and volume-of-interest (VOI) automatically removing hyperintense non-brain fat/muscle tissue with MRICron tool (<http://www.mricron.com>) (Smith 2002). Next, tissue-type segmentation was carried out using the FSL FAST4 tool.

Both gray and white-matter partial volume images were aligned to MNI152 standard space using the affine registration FSL tool FLIRT, followed by non-linear registration

using FNIRT, which uses a b-spline representation of the registration warp field. The resulting images were averaged to create a study-specific template, including a randomly chosen equally represented subgroup patient subset, to which the native images were then non-linearly re-registered. To minimize T1 sequence variability across centers and between 3T and 1.5T scanner, spatially varying noise patterns due to field inhomogeneity were corrected using FSL's SUSAN noise reduction pipeline, which reduce noise in an image using non-linear filtering (Smith and Brady 1997). The registered partial volume image intensities were then modulated to correct for local expansion or contraction. The modulated segmented images were smoothed with an isotropic Gaussian kernel with a sigma of 4 mm. Sample homogeneity, implemented in CAT12 SPM toolbox (<http://dbm.neuro.uni-jena.de/cat/>), was checked using covariance matrix to identify potential outliers. Partial correlation analysis was run, including age, gender, and eTIV as nuisance variables. Participants were excluded if covariance was less than 2 SD below the sample mean.

In the following statistical non-parametric analysis, particular attention was paid to the used masks to better define brainstem structure and avoid gray/white-matter misassignment due to the partial volume effect. The gray-matter VBM mean template was binarized using 0.2 fractional intensity value as threshold for gray-matter inclusion. White-matter VBM mask was obtained based on fractional anisotropy (FA) mean template. Namely, in a subsample of MSA patients studied in Venice, FA was calculated with the Freesurfer DT-recon tool, after motion and eddy-current correction. A study-specific FA template was created using the FA images from all participants (Abe et al. 2010). Then, all participants' FA images were coregistered to the standard space FA template provided by FSL (FMRIB58_1 mm) using an affine 12-parameter transformation, followed by a non-linear transformation. The resulting normalized FA images were then smoothed with an 8 mm isotropic Gaussian kernel, and a mean image (FA template) was created. Individual participants' FA images were then registered to the customized FA template using the FSL registration tool using Tract-Based Spatial Statistics (TBSS) preprocessing routine. Mean FA template was then binarized using 0.3 fractional anisotropy value as conservative threshold for white-matter inclusion.

Full-automated subcortical volume segmentation

Subcortical brain volumes were calculated from MRI T1-3D using the software package FreeSurfer (version 6.00b), which is freely available in online at <http://surfer.nmr.mgh.harvard.edu/> and has a specialized tool for automated parcellation of the neocortical gray-matter and

subcortical volumes (Dale et al. 1999; Fischl et al. 1999). Mapping between participants and the atlas was performed using a non-rigid registration on the inflated surface. The end-result is the parcellation of the human cortex into 34 cortical regions of interest in each hemisphere and into 19 subcortical white-matter and deep gray-matter volumetric structures (Desikan et al. 2006). Moreover, the new Bayesian-based brainstem segmentation routine was used to obtain volumes of the superior cerebellum peduncles, pons, midbrain, and medulla (Iglesias et al. 2015). For the purpose of the study, only subcortical volume measures were included as factor in model analysis. An overall mean left and right hemisphere index was calculated after pairwise *T* test to verify the absence of significant between-hemisphere differences for each subcortical structure.

Statistical analysis

We used the Chi-square test to assess differences in the distribution of categorical variables between the whole MSA sample versus HC as well as between MSA-NC and MSA-CI. Continuous clinical and demographic variables in the same groups were compared with Mann–Whitney *U* test adjusted with bootstrap (1000 iterations to reduce false positives).

Voxelwise VBM general linear model (GLM) analysis was run using FSL's "randomize" tool to compare MSA versus HC with the following covariates: age, education, gender, and intracranial volume calculated as estimated total intracranial volume (eTIV). Age, education, MDS-UPDRS III, scanning sites, and eTIV were used as covariates in MSA-CI versus MSA-NC comparisons. Finally, non-parametric statistics were performed using the FSL "randomize" tool with 15,000 permutations, correcting for multiple comparisons across space using threshold-free cluster enhancement (TFCE) option either enabled or disabled (i.e., voxel-based thresholding without the TFCE option in randomize is uncorrected for multiple comparisons), using previously calculated gray- and white-matter masks.

To obtain anatomical localization of statistical results of gray and white matter, the Automated Anatomical Labeling template and the Johns Hopkins University white-matter tractography atlas were used, respectively (Mori et al. 2005; Rolls et al. 2015).

GLM multivariate analyses were used to compare MSA versus HC and MSA-CI versus MSA-NC subcortical volumes obtained with full-automated segmentation, taking into account the same covariates of the previous analysis. Sidak correction for multiple comparisons was also performed. The statistical analysis was carried out using SPSS 20.0.

Results

Demographic and clinical details of MSA as a whole group, as well as HC and MSA subgroups (MSA-NC and MSA-CI) are shown in Table 1. MSA and HC groups were matched for each variable, except for MMSE, which was significantly lower in MSA patients. Compared with the MSA-NC, the MSA-CI patients were older, had lower education, and showed a trend for older age at onset.

No participant was excluded from the analysis after the sample homogeneity check. VBM analysis revealed gray-matter volume thinning in several regions most prominent in the cerebellum, and the frontal, the parietal, and the occipital lobes and partially in the temporal lobe compared with HC. Moreover, gray-matter reductions were found bilaterally in the putamen and in the middle cingulate gyri. In addition, we found that volume increases bilaterally in the occipital gray matter (namely, anterior lingual gyrus and calcarine cortex), in right amygdala, periaqueductal gray (PAG), and in the posterior thalamus, caudate nucleus, and olfactory cortex (Table 2a; Fig. 1). White-matter volume thinning was present mainly in the cerebellum bilaterally, anterior thalamic radiation, cingulum, and corpus callosum (Table 2c; Fig. 1).

The MSA-CI versus MSA-NC VBM comparison showed selective gray-matter thinning only in the left dorsolateral prefrontal cortex (DLPFC) of MSA-CI (Table 2b; Fig. 2).

Analysis of subcortical volumes segmentation showed numerous volume reductions in MSA versus HC, particularly in medulla, pons, superior cerebellar peduncles, midbrain, middle posterior corpus callosum, cerebellar white and gray matter, putamen, globus pallidus, nucleus accumbens, thalamus, and ventral diencephalon (Online Resource 3). The direct comparison MSA-CI versus MSA-NC group showed no significant volumetric differences in subcortical structures.

Discussion

In the present multicenter study, MSA patients showed widespread thinning in cortical brain regions (bilateral frontal, occipito-temporal, and parietal areas), white-matter thinning, and subcortical alterations. Moreover, the presence of cognitive impairment in MSA was associated with focal reduction in the left DLPFC volume.

The finding of frontal involvement is in line with other imaging studies showing MSA cognitive dysfunctions

Table 1 Demographic and clinical characteristics of HC and MSA subgroups

	MSA (<i>n</i> = 72)		HC (<i>n</i> = 36)		MSA-NC (<i>n</i> = 50)		MSA-CI (<i>n</i> = 22)		MSA vs. HC <i>P</i> value	MSA-NC vs. MSA-CI <i>P</i> value
	Mean (SD)	Mdn	Mean (SD)	Mdn	Mean (SD)	Mdn	Mean (SD)	Mdn		
Age ^a (years)	63.8 (6.8)	64	61.6 (7.4)	62.0	62.6 (6.6)	62.0	66.4 (6.5)	67.5		*
Education ^a (years)	11.2 (4.7)	11	12.5 (4.5)	13.0	12.4 (4.5)	12.0	8.4 (4.1)	8.0		**
Gender ^b (male/female)	29/43		21/15		22/28		7/15			
Age of onset ^a (years)	59.0 (7.2)	60			58.0 (7.0)	58.0	61.3 (7.2)	62.0		*
Disease duration ^a (years)	4.6 (3.0)	4			4.4 (2.9)	4.0	5.1 (3.3)	4.0		
MMSE ^a	26.7 (3.1)	28	29.1 (1.0)	29.0	28.4 (1.1)	28.0	22.8 (2.7)	23.0	***	***
MDS-UPDRS III ^a	41.3 (14.9)	41			39.7 (16.1)	41.0	44.9 (11.4)	42.0		
MSA-C/MSA-P ^b	25/47				18/32		7/15			
Center (1/2/3/4/5) ^b	34/18/6/7/7		36/0/0/0/0		21/14/6/7/2		13/4/0/0/5		***	*
eTIV ^a	1463.7 (160.0)	1436.8	1439.8 (178.7)	1441.4	1477.0 (170.7)	1447.3	1433.7 (131.2)	1423.6		

Centers: 1 = Venice (IT), 2 = Innsbruck (A), 3 = New York (USA), 4 = Bologna (IT), 5 = Chieti (IT)

MSA multiple system atrophy, HC healthy controls, MSA-NC MSA with normal cognition, MSA-CI MSA with cognitive impairment, SD standard deviation, Mdn median, MMSE Mini-Mental State Examination, MDS-UPDRS III Movement Disorder Society Unified Parkinson Disease Rating Scale, eTIV estimated total intracranial volume

* $P < 0.05$; ** $P < 0.01$; *** $P < 0.001$

^a Mann-Whitney *U* test non-parametric was used for continuous variable between MSA and HC

^b Pearson Chi-squared test was used to assess differences in the distribution and percentage of categorical variables among MSA, HC, and MSA subgroups

Table 2 Voxel-based morphometry gray- and white-matter difference

GM VBM	AAL2 atlas	Voxels ^a	Z score	P value	X (mm) (MNI)	Y (mm) (MNI)	Z (mm) (MNI)	Side
(a) MSA < HC	Cerebellum VIII	5614	9.5	<0.00001	-22	-54	-46	Left
	Cerebellum VIII		9.3		22	-58	-46	Right
	Cerebellum IX		7.7		-18	-50	-46	Left
	Cerebellum IX		5.3		18	-46	-46	Right
	Cerebellum VIIb		6.4		-14	-76	-46	Left
	Cerebellum VIIb		6.5		18	-74	-46	Right
	Cerebellum crus II		6.3		-30	-74	-46	Left
	Cerebellum crus II		5.5		30	-78	-42	Right
	Cerebellum VI		5.7		-30	-60	-26	Left
	Cerebellum VI		5.9		26	-60	-30	Right
	Cerebellum (vermis)		6.8		0	-62	-26	Midline
	Fusiform		5.3		-30	-58	-8	Left
	Supramarginal	452	6.1	<0.00001	-64	-20	38	Left
	Precentral	59	5.2	<0.00001	-26	-20	68	Left
	Postcentral	55	5.0	<0.00001	-58	-2	40	Left
	Middle cingulate	33	5.5	<0.00001	-14	-42	36	Left
	Putamen	40	6.2	<0.00001	-26	2	12	Left
	Inferior frontal	20	4.8	<0.00001	-40	10	24	Left
	Middle occipital	3	4.6	<0.00001	-20	-90	-2	Left
	Lingual	1	4.6	<0.00001	-16	-82	0	Left
	Inferior Occipital	1	4.6	<0.00001	-24	-90	-6	Left
	Lingual	28	5.3	<0.00001	20	-76	-2	Right
	Inferior temporal	27	5.4	<0.00001	50	-44	-14	Right
	Middle temporal	25	5.0	<0.00001	52	-30	-10	Right
	Putamen	112	6.0	<0.00001	28	0	12	Right
	Middle cingulate	67	5.4	<0.00001	16	-34	38	Right
	Precentral	63	5.1	<0.00001	56	2	42	Right
	Inferior frontal	60	4.8	<0.00001	52	14	26	Right
	Superior frontal	17	4.9	<0.00001	32	-8	66	Right
	Fusiform	9	4.9	<0.00001	32	-66	-6	Right
	Angular	3	4.7	<0.00001	44	-50	30	Right
	MSA > HC	Thalamus		8.6	<0.00001	-6	-28	0
Amygdala		10	4.9	<0.00001	20	-2	-14	Right
Thalamus		4081	11.7	<0.00001	6	-24	16	Right
Thalamus			6.9		-8	-18	10	Left
Olfactory			8.3		6	10	-14	Right
Olfactory			5.2		-8	16	-14	Left
Periaqueductal gray			4.3	<0.00001	2	-22	-16	Right
Calcarine		1173	6.7	<0.00001	2	-70	10	Right
Calcarine			6.0		-5	-72	10	Left
Lingual			5.9		6	-60	2	Right
Lingual		19	5.0	<0.00001	-10	-40	-4	Left
(b) MSA-CI < MSA-NC	Middle frontal	572	3.80	0.00007	-32	26	44	Left
WM VBM	JHU white-matter atlas	Voxels ^a	Z score	P value	X (mm) (MNI)	Y (mm) (MNI)	Z (mm) (MNI)	Side
(c) MSA < HC	Anterior thalamic radiation	10,143	15.9	<0.00001	-18	-2	0	Left
	Anterior thalamic radiation		16.3		18	-4	0	Right
	Cerebellum white matter		12.0		-4	-56	-16	Left
	Cerebellum white matter		13.4		4	-56	-16	Right

Table 2 continued

WM VBM	JHU white-matter atlas	Voxels ^a	Z score	P value	X (mm) (MNI)	Y (mm) (MNI)	Z (mm) (MNI)	Side
	Corticospinal tract		10.3		4	-30	-40	Right
	Superior longitudinal fasciculus		9.5		32	-8	6	Right
	Cingulum	1565	6.9	<0.00001	-6	-38	30	Left
	Splenium of corpus callosum		6.0		-6	-40	24	Left
	Body of corpus callosum		4.8		-4	-28	18	Left
	Cingulum		6.2		14	-16	36	Right
	Cingulum (cingulate gyrus)	22	5.3	<0.00001	-4	2	34	Left
	Inferior longitudinal fasciculus	12	3.9	0.00005	-48	-16	-16	Left
	Cingulum (hippocampus)	55	7.6	<0.00001	24	-30	-12	Right
	Body of corpus callosum	40	5.0	<0.00001	4	-16	28	Right
	Inferior fronto-occipital fasciculus	17	4.3	<0.00001	18	34	-16	Right
	Uncinate fasciculus	2	4.5	<0.00001	18	10	-14	Right
	Fornix	1	5.2	<0.00001	4	-2	-8	Left
	Callosal body posterior pars	1	3.6	0.0002	-2	-24	20	Left
	Callosal body posterior pars	1	3.5	0.0002	2	-24	20	Right

GM gray matter, WM white matter, VBM voxel-based morphometry, MNI Montreal Neurological Institute, AAL2 new anatomical automatic labeling. JHU Johns Hopkins University, MSA multiple system atrophy, HC healthy controls, MSA-NC MSA with normal cognition, MSA-CI MSA with cognitive impairment

^a Image was overlaid into MNI $2 \times 2 \times 2$ mm³ template

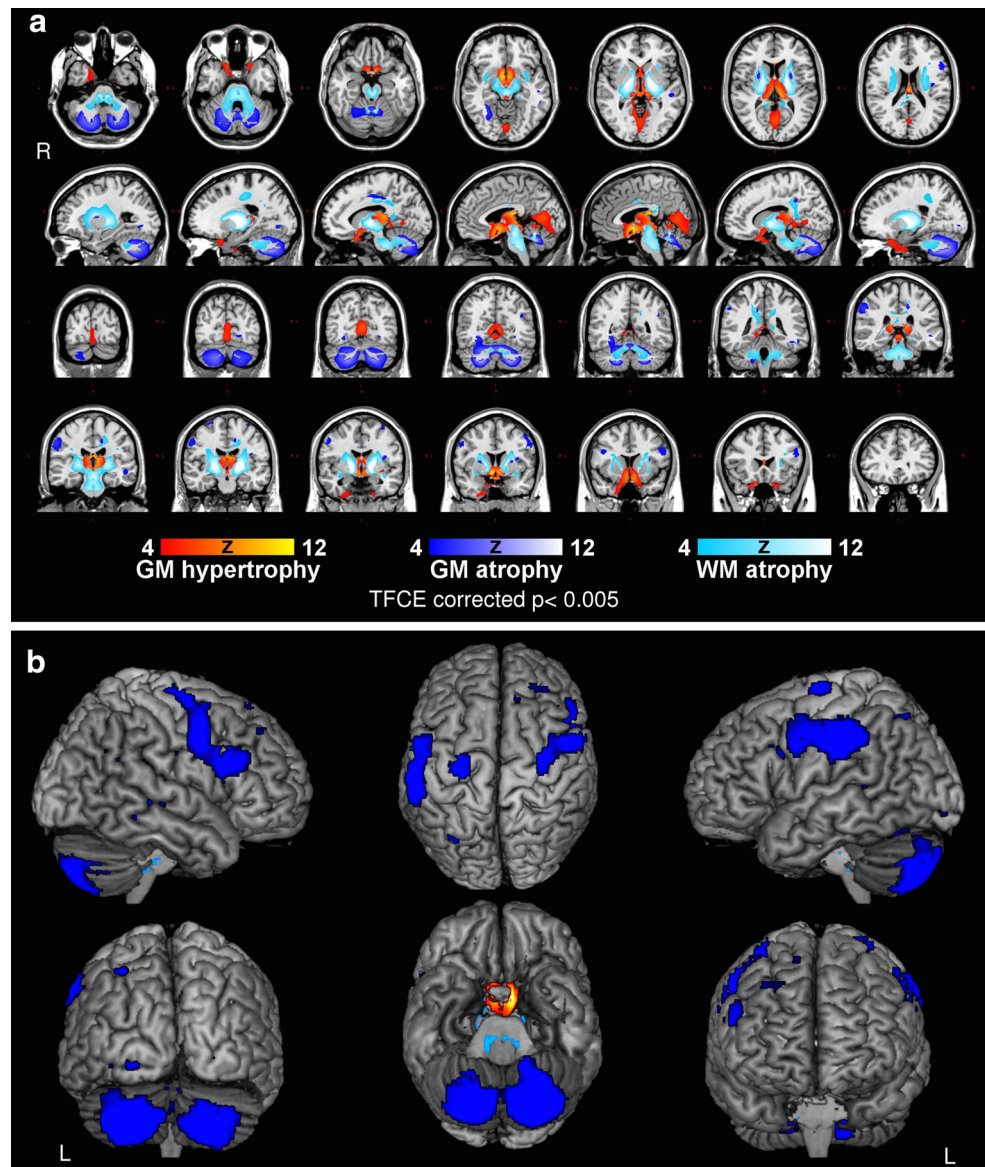
associated with frontal hypometabolism, hypoperfusion (Kawai et al. 2008; Kitayama et al. 2009; Lyoo et al. 2008) and neuronal loss in the frontal region (Salvesen et al. 2015). Moreover, our results of specific frontal alterations in MSA-CI are in agreement with our previous neuropsychological studies, showing the predominance of fronto-executive deficits (Auzou et al. 2015; Siri et al. 2013; Stankovic et al. 2014). These results suggest a different pattern of cortical changes from cognitively impaired Parkinson patients (PD), where widespread gray-matter cortical atrophy is consistently reported (Biundo et al. 2016). In this regard, it is conceivable that MSA and PD cognitive manifestations are associated with distinct underlying mechanisms. Focal fronto-striatal alterations dominate in MSA, consistently with the concept of “subcortical dementia”, which is characterized by executive dysfunctions, slow information processing, and retrieval-type memory deficits as well as impairment in cognitive skills based on frontal network functioning (Brown and Marsden 1988; Cummings 1986; Stankovic et al. 2014; Tekin and Cummings 2002).

Our results are in line with these subcortical alterations and corroborate data from our previous study on MSA performance in MMSE scale subitems (Fiorenzato et al. 2016). In particular, our MSA-CI subgroup showed deficits in executive (namely, “calculation”) memory retrieval (namely, “retrieval of three words”) and visuoconstructive subitems (“copy pentagons”). This latter finding should also be interpreted as consequence of

frontal involvement in the execution of the copy of pentagons (Filoteo et al. 2014). Indeed, in another cohort, we demonstrated severely impaired default mode network connectivity in MSA consistent with prominent frontal involvement and secondary to basal ganglia alterations (Franciotti et al. 2015). However, since the natural motor course of MSA usually affects daily functioning, it is difficult to determine if subcortical cognitive dysfunctions are by themselves sufficient to impair functional independence. Therefore, we propose to avoid the term “subcortical dementia”.

The findings of widespread brain alteration in MSA in comparison with controls expand previous VBM findings (Brenneis et al. 2003; Chang et al. 2009; Minnerop et al. 2007, 2010; Shigemoto et al. 2013), considering also the larger sample size of our cohort. In addition, by applying a fully automated segmentation method, we detected atrophy in the midbrain, pons, medulla oblongata, and superior cerebellar peduncle. Moreover, in agreement with previous studies, there were further significant volume reductions in the putamen and in the cerebellum but interestingly not in the caudate nucleus (Messina et al. 2011; Scherfler et al. 2016). This finding has been reported in other neuroimaging and neuropathological studies. Indeed, degeneration in the caudate nucleus could be mild or absent even in severe MSA and most importantly is less prominent than in the putamen (Barbagallo et al. 2016; Wenning et al. 1997), whose role in motor control has been extensively reported (Alexander et al. 1986).

Fig. 1 Voxel-based morphometry comparison between MSA and HC. **a** Axial view; **b** 3D view. A statistical threshold $Z < 4$ was used for visualization purpose. *MSA* multiple system atrophy, *HC* healthy controls, *GM* gray matter, *WM* white matter, *TFCE* Threshold-Free Cluster Enhancement

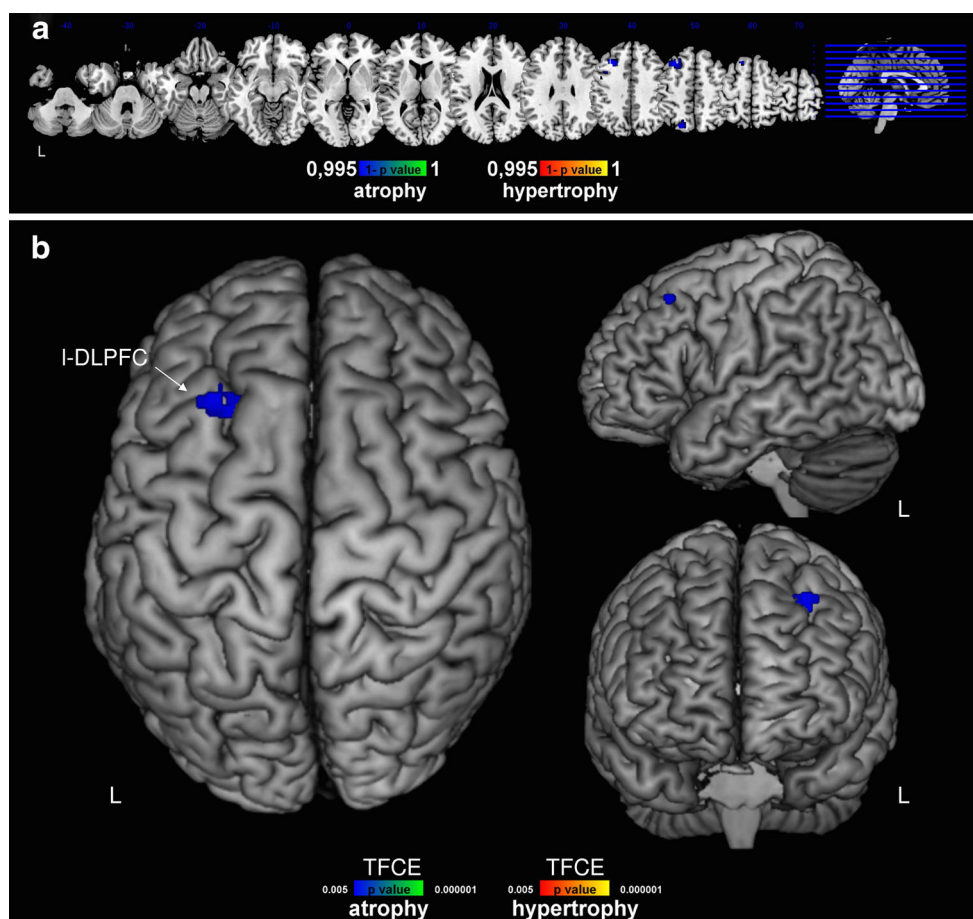


We also found white-matter reductions in the cerebellum, anterior thalamic radiation, corticospinal tract, and corpus callosum consistently with previous studies, suggesting that these tracts are specifically affected by the disease process (Minnerop et al. 2010; Shigemoto et al. 2013; Worker et al. 2014). Finally, we also identified volume increases in the occipital lobes bilaterally (anterior lingual gyrus and calcarine cortex), posterior thalamus, nucleus caudate, olfactory cortex, right amygdala, and PAG, which we believe to be related to microstructural changes and remodeling and secondary to the pathological processes. Gray-matter volume increases have been reported in other neurodegenerative disorders, including early stage of Alzheimer (AD) and Huntington disease, where cortical and subcortical volume increases may precede atrophies, characteristic of more advanced patients

(Fortea et al. 2011; Rosas et al. 2008). These areas of relative volume increase may be related to reactive neuronal hypertrophy and/or local inflammation (Fortea et al. 2010). In the thalamus, we found a conflicting result of volume reduction with full-segmented analysis and volume increases (in the posterior region) in VBM. This may be explained by the lower accuracy of VBM compared to the fully automated subcortical segmentation in the analysis of subcortical structures located near the ventricles, such as the thalamus (Schwarz et al. 2014).

Our retrospective multicenter study has some weaknesses. We could not identify MSA cognitive subgroups based on an extensive neuropsychological examination, but considered only the total raw score of the MMSE, which, as brief cognitive scale, has limitations. Nevertheless, we applied an MMSE cut-off score (< 27) that we have

Fig. 2 Voxel-based morphometry comparison between MSA-CI and MSA-NC. **a** Uncorrected (P value < 0.005) maps; **b** axial and 3D views. *MSA* multiple system atrophy, *MSA-CI* MSA with cognitive impairment, *MSA-NC* MSA with normal cognition, *TFCE* Threshold-Free Cluster Enhancement, *I-DLPFC*: left dorsolateral prefrontal cortex



recently validated using an extensive neuropsychological battery, which was not possible to obtain for all patients in the current study given its retrospective design. Second, we could enroll healthy controls only at Venice center and we collected data using 1.5T and 3T MRI. However, we checked the homogeneity of our sample and there were no outliers; moreover, we performed a field homogeneity correction and included the centers as covariates in VBM analysis.

In conclusion, our results corroborate previous evidence reporting broad cortical and subcortical alterations in MSA relative to HC, also indicating the crucial contribution of white-matter involvement. Given the neuroanatomical pattern involving white and gray-matter cortical and subcortical structures, physicians should consider the heterogeneous nature of this pathology. Moreover, the presence of significant MMSE abnormalities associated with focal volume reduction in the left DLPFC suggests in MSA only a marginal contribution of cortical pathology to cognitive defects, a condition which is very different from other neurodegenerative diseases, such as AD or PD. Cognitive dysfunction seems associated with disruption of the striato-pallido-thalamo-cortical circuits, in which cortical deficits are secondary to subcortical alterations. Finally, our

findings should encourage listing the presence of specific fronto-striatal features among the consensus criteria for MSA diagnosis (Gilman et al. 2008).

Acknowledgements The authors thank the MSA patients who kindly participated in this study.

Compliance with ethical standards

All authors gave the final approval of this version of the manuscript to be published. We can assure that there is no one else who fulfills the criteria but has not been included as an author.

Ethical approval All procedures performed in this study were in accordance with the ethical standards of the Venice Research Ethics Committee (Venice, Italy) and with the 1964 Helsinki declaration. For this type of study, formal consent is not required.

Conflict of interest The authors have no competing interest to declare.

References

- Abe O, Takao H, Gono W, Sasaki H, Murakami M, Kabasawa H, Kawaguchi H, Goto M, Yamada H, Yamasue H, Kasai K, Aoki S, Ohtomo K (2010) Voxel-based analysis of the diffusion tensor. *Neuroradiology* 52(8):699–710

- Alexander GE, DeLong MR, Strick PL (1986) Parallel organization of functionally segregated circuits linking basal ganglia and cortex. *Annu Rev Neurosci* 9:357–381
- Antonini A, Kazumata K, Feigin A, Mandel F, Dhawan V, Margoulef C, Eidelberg D (1998) Differential diagnosis of parkinsonism with [¹⁸F] fluorodeoxyglucose and PET. *Mov Disord* 13(2):268–274
- Asi YT, Ling H, Ahmed Z, Lees AJ, Revesz T, Holton JL (2014) Neuropathological features of multiple system atrophy with cognitive impairment. *Mov Disord* 29(7):884–888
- Auzou N, Dujardin K, Biundo R, Foubert-Samier A, Barth C, Duval F, Tison F, Defebvre L, Antonini A, Meissner WG (2015) Diagnosing dementia in multiple system atrophy by applying Movement Disorder Society diagnostic criteria for Parkinson's disease dementia. *Parkinsonism Relat Disord* 21(10):1273–1277
- Barbagallo G, Sierra-Pena M, Nemmi F, Traon AP, Meissner WG, Rascol O, Peran P (2016) Multimodal MRI assessment of nigrostriatal pathway in multiple system atrophy and Parkinson disease. *Mov Disord* 31(3):325–334
- Biundo R, Weis L, Antonini A (2016) Cognitive decline in Parkinson's disease: the complex picture. *NPJ Parkinsons Dis* 2:16018
- Brenneis C, Seppi K, Schocke MF, Muller J, Luginger E, Bosch S, Loscher WN, Buchel C, Poewe W, Wenning GK (2003) Voxel-based morphometry detects cortical atrophy in the Parkinson variant of multiple system atrophy. *Mov Disord* 18(10):1132–1138
- Brown RG, Marsden CD (1988) 'Subcortical dementia': the neuropsychological evidence. *Neuroscience* 25(2):363–387
- Chang CC, Chang YY, Chang WN, Lee YC, Wang YL, Lui CC, Huang CW, Liu WL (2009) Cognitive deficits in multiple system atrophy correlate with frontal atrophy and disease duration. *Eur J Neurol* 16(10):1144–1150
- Ciulli L, Krismer F, Nicoletti F, Wenning GK (2014) An update on the cerebellar subtype of multiple system atrophy. *Cerebellum Ataxias* 1:14
- Colosimo C, Vanacore N, Bonifati V, Fabbrini G, Rum A, De Michele G, De Mari M, Bonuccelli U, Nicholl DJ, Meco G (2001) Clinical diagnosis of multiple system atrophy: level of agreement between Quinn's criteria and the consensus conference guidelines. *Acta Neurol Scand* 103(4):261–264
- Cummings JL (1986) Subcortical dementia. *Neuropsychology, neuropsychiatry, and pathophysiology*. *Br J Psychiatry* 149(6):682–697
- Dale AM, Fischl B, Sereno MI (1999) Cortical surface-based analysis. I. Segmentation and surface reconstruction. *Neuroimage* 9(2):179–194
- Desikan RS, Segonne F, Fischl B, Quinn BT, Dickerson BC, Blacker D, Buckner RL, Dale AM, Maguire RP, Hyman BT, Albert MS, Killiany RJ (2006) An automated labeling system for subdividing the human cerebral cortex on MRI scans into gyral based regions of interest. *Neuroimage* 31(3):968–980
- Filoteo JV, Reed JD, Litvan I, Harrington DL (2014) Volumetric correlates of cognitive functioning in nondemented patients with Parkinson's disease. *Mov Disord* 29(3):360–367
- Fiorenzato E, Weis L, Falup-Pecurariu C, Diaconu S, Siri C, Reali E, Pezzoli G, Bisiacchi P, Antonini A, Biundo R (2016) Montreal Cognitive Assessment (MoCA) and Mini-Mental State Examination (MMSE) performance in progressive supranuclear palsy and multiple system atrophy. *J Neural Transm*. doi:10.1007/s00702-016-1589-3
- Fischl B, Sereno MI, Dale AM (1999) Cortical surface-based analysis. II: Inflation, flattening, and a surface-based coordinate system. *Neuroimage* 9(2):195–207
- Folstein MF, Folstein SE, McHugh PR (1975) Mini-mental state. *J Psychiatr Res* 12(3):189–198
- Fortea J, Sala-Llonch R, Bartres-Faz D, Bosch B, Llado A, Bargallo N, Molinuevo JL, Sanchez-Valle R (2010) Increased cortical thickness and caudate volume precede atrophy in PSEN1 mutation carriers. *J Alzheimers Dis* 22(3):909–922
- Fortea J, Sala-Llonch R, Bartres-Faz D, Llado A, Sole-Padullés C, Bosch B, Antonell A, Olives J, Sanchez-Valle R, Molinuevo JL, Rami L (2011) Cognitively preserved subjects with transitional cerebrospinal fluid ss-amyloid 1-42 values have thicker cortex in Alzheimer's disease vulnerable areas. *Biol Psychiatry* 70(2):183–190
- Franciotti R, Delli Pizzi S, Perfetti B, Tartaro A, Bonanni L, Thomas A, Weis L, Biundo R, Antonini A, Onofri M (2015) Default mode network links to visual hallucinations: a comparison between Parkinson's disease and multiple system atrophy. *Mov Disord* 30(9):1237–1247
- Gilman S, Wenning GK, Low PA, Brooks DJ, Mathias CJ, Trojanowski JQ, Wood NW, Colosimo C, Durr A, Fowler CJ, Kaufmann H, Klockgether T, Lees A, Poewe W, Quinn N, Revesz T, Robertson D, Sandroni P, Seppi K, Vidailhet M (2008) Second consensus statement on the diagnosis of multiple system atrophy. *Neurology* 71(9):670–676
- Iglesias JE, Van Leemput K, Bhatt P, Casillas C, Dutt S, Schuff N, Truran-Sacrey D, Boxer A, Fischl B, Alzheimer's Disease Neuroimaging I (2015) Bayesian segmentation of brainstem structures in MRI. *Neuroimage* 113:184–195
- Jenkinson M, Beckmann CF, Behrens TE, Woolrich MW, Smith SM (2012) Fsl. *Neuroimage* 62(2):782–790
- Kawai Y, Suenaga M, Takeda A, Ito M, Watanabe H, Tanaka F, Kato K, Fukatsu H, Naganawa S, Kato T, Ito K, Sobue G (2008) Cognitive impairments in multiple system atrophy: MSA-C vs MSA-P. *Neurology* 70:1390–1396
- Kim JS, Yang JJ, Lee DK, Lee JM, Youn J, Cho JW (2015) Cognitive impairment and its structural correlates in the Parkinsonian subtype of multiple system atrophy. *Neurodegener Dis* 15(5):294–300
- Kitayama M, Wada-Isoe K, Irizawa Y, Nakashima K (2009) Assessment of dementia in patients with multiple system atrophy. *Eur J Neurol* 16(5):589–594
- Lee MJ, Shin JH, Seoung JK, Lee JH, Yoon U, Oh JH, Jung DS, Kim EJ (2016) Cognitive impairments associated with morphological changes in cortical and subcortical structures in multiple system atrophy of the cerebellar type. *Eur J Neurol* 23(1):92–100
- Lyoo CH, Jeong Y, Ryu YH, Lee SY, Song TJ, Lee JH, Rinne JO, Lee MS (2008) Effects of disease duration on the clinical features and brain glucose metabolism in patients with mixed type multiple system atrophy. *Brain* 131:438–446
- Messina D, Cerasa A, Condino F, Arabia G, Novellino F, Nicoletti G, Salsone M, Morelli M, Lanza PL, Quattrone A (2011) Patterns of brain atrophy in Parkinson's disease, progressive supranuclear palsy and multiple system atrophy. *Parkinsonism Relat Disord* 17(3):172–176
- Minnerop M, Specht K, Ruhlmann J, Schimke N, Abele M, Weyer A, Wullner U, Klockgether T (2007) Voxel-based morphometry and voxel-based relaxometry in multiple system atrophy—a comparison between clinical subtypes and correlations with clinical parameters. *Neuroimage* 36(4):1086–1095
- Minnerop M, Luders E, Specht K, Ruhlmann J, Schimke N, Thompson PM, Chou YY, Toga AW, Abele M, Wullner U, Klockgether T (2010) Callosal tissue loss in multiple system atrophy—a one-year follow-up study. *Mov Disord* 25(15):2613–2620
- Mori S, Wakana S, Van Zijl PCM, Nagae-Poetscher LM (2005) MRI atlas of human white matter. Elsevier, Amsterdam
- Quinn N (1989) Multiple system atrophy—the nature of the beast. *J Neurol Neurosurg Psychiatry* 52(Suppl):78–89

- Rolls ET, Joliot M, Tzourio-Mazoyer N (2015) Implementation of a new parcellation of the orbitofrontal cortex in the automated anatomical labeling atlas. *Neuroimage* 122:1–5
- Rosas HD, Salat DH, Lee SY, Zaleta AK, Pappu V, Fischl B, Greve D, Hevelone N, Hersch SM (2008) Cerebral cortex and the clinical expression of Huntington's disease: complexity and heterogeneity. *Brain* 131(4):1057–1068
- Salvesen L, Winge K, Brudek T, Agander TK, Lokkegaard A, Pakkenberg B (2015) Neocortical neuronal loss in patients with multiple system atrophy: a stereological study. *Cereb Cortex*. doi:10.1093/cercor/bhv228
- Scherfner C, Gobel G, Muller C, Nocker M, Wenning GK, Schocke M, Poewe W, Seppi K (2016) Diagnostic potential of automated subcortical volume segmentation in atypical parkinsonism. *Neurology* 86(13):1242–1249
- Schmidt R, Enzinger C, Ropele S, Schmidt H, Fazekas F (2003) Progression of cerebral white matter lesions: 6-year results of the Austrian Stroke Prevention Study. *The Lancet* 361(9374):2046–2048
- Schwarz CG, Reid RI, Gunter JL, Senjem ML, Przybelski SA, Zuk SM, Whitwell JL, Vemuri P, Josephs KA, Kantarci K, Thompson PM, Petersen RC, Jack CR Jr, Alzheimer's Disease Neuroimaging Initiative (2014) Improved DTI registration allows voxel-based analysis that outperforms tract-based spatial statistics. *Neuroimage* 94:65–78
- Shigemoto Y, Matsuda H, Kamiya K, Maikusa N, Nakata Y, Ito K, Ota M, Matsunaga N, Sato N (2013) In vivo evaluation of gray and white matter volume loss in the parkinsonian variant of multiple system atrophy using SPM8 plus DARTEL for VBM. *Neuroimage Clin* 2:491–496
- Siri C, Duerr S, Canesi M, Delazer M, Esselink R, Bloem BR, Gurevich T, Balas M, Giladi N, Santacruz P, Marti F, Tolosa E, Rubino A, Meco G, Poewe W, Pezzoli G, Wenning G, Antonini A (2013) A cross-sectional multicenter study of cognitive and behavioural features in multiple system atrophy patients of the parkinsonian and cerebellar type. *J Neural Transm (Vienna)* 120(4):613–618
- Smith SM (2002) Fast robust automated brain extraction. *Hum Brain Mapp* 17(3):143–155
- Smith SM, Brady JM (1997) SUSAN—A new approach to low level image processing. *Int J Comput Vis* 23(1):45–78
- Stankovic I, Krismer F, Jesic A, Antonini A, Benke T, Brown RG, Burn DJ, Holton JL, Kaufmann H, Kostic VS, Ling H, Meissner WG, Poewe W, Semnic M, Seppi K, Takeda A, Weintraub D, Wenning GK, Movement Disorders Society MSASG (2014) Cognitive impairment in multiple system atrophy: a position statement by the neuropsychology task force of the MDS multiple system atrophy (MODIMSA) study group. *Mov Disord* 29(7):857–867
- Tekin S, Cummings JL (2002) Frontal–subcortical neuronal circuits and clinical neuropsychiatry. *J Psychosom Res* 53(2):647–654
- Wenning GK, Ben-Shlomo Y, Magalhaes M, Daniel SE, Quinn NP (1995) Clinicopathological study of 35 cases of multiple system atrophy. *J Neurol Neurosurg Psychiatry* 58(2):160–166
- Wenning GK, Tison F, Ben Shlomo Y, Daniel SE, Quinn NP (1997) Multiple system atrophy: a review of 203 pathologically proven cases. *Mov Disord* 12(2):133–147
- Worker A, Blain C, Jarosz J, Chaudhuri KR, Barker GJ, Williams SC, Brown RG, Leigh PN, Dell'Acqua F, Simmons A (2014) Diffusion tensor imaging of Parkinson's disease, multiple system atrophy and progressive supranuclear palsy: a tract-based spatial statistics study. *PLoS One* 9(11):e112638